AD_____

Award Number: DAMD17-99-1-9444

TITLE: Rational Derivatives of Maspin as Candidate Tumor Suppressive Agents of Breast Cancer

PRINCIPAL INVESTIGATOR: Shihie Sheng, Ph.D.

CONTRACTING ORGANIZATION: Wayne State University
Detroit, Michigan 48201-1379

REPORT DATE: August 2000

TYPE OF REPORT: Annual

PREPARED FOR: U.S. Army Medical Research and Materiel Command
Fort Detrick, Maryland 21702-5012

REPORT DOCUMENTATION PAGE

Form Approved
OMB No. 074-0188

1. AGENCY USE ONLY (Leave blank)	2. REPORT DATE	3. REPORT TYPE AND DATES COVERED
	August 2000	Annual (1 Jul 99 - 1 Jul 00)

4. TITLE AND SUBTITLE

Rational Derivatives of Maspin as Candidate Tumor Suppressive Agents of Breast Cancer

5. FUNDING NUMBERS

DAMD17-99-1-9444

6. AUTHOR(S)

Shihie Sheng, Ph.D.

7. PERFORMING ORGANIZATION NAME(S) AND ADDRESS(ES)

Wayne State University
Detroit, Michigan 48201-1379

8. PERFORMING ORGANIZATION REPORT NUMBER

9. SPONSORING / MONITORING AGENCY NAME(S) AND ADDRESS(ES)

U.S. Army Medical Research and Materiel Command
Fort Detrick, Maryland 21702-5012

10. SPONSORING / MONITORING AGENCY REPORT NUMBER

11. SUPPLEMENTARY NOTES

12a. DISTRIBUTION / AVAILABILITY STATEMENT

Approved for Public Release; Distribution Unlimited

12b. DISTRIBUTION CODE

13. ABSTRACT *(Maximum 200 Words)*

14. SUBJECT TERMS

breast cancer

15. NUMBER OF PAGES

11

16. PRICE CODE

17. SECURITY CLASSIFICATION OF REPORT	18. SECURITY CLASSIFICATION OF THIS PAGE	19. SECURITY CLASSIFICATION OF ABSTRACT	20. LIMITATION OF ABSTRACT
Unclassified	Unclassified	Unclassified	Unlimited

Table of Contents

Annual Report for the period of 7/1/00-6/30/01

We proposed to generate and characterize six rational derivatives of maspin as candidate tumor suppressive agents of breast cancer. We plan to produce these novel maspin variants as purified proteins (**Specific Objective 1**), and as re-expressed proteins in breast tumor cells that are transfected with the corresponding coding cDNAs (**Specific Objective 2**). The biological functions of these six maspin derivatives as well as the wild type maspin will be examined using comprehensive cellular and biochemical assays that have been established in my laboratory. In particular, I will focus on the effect of these molecules on tumor growth, cell adhesion, cell motility and invasion. In addition the biochemical and biophysical properties of these new molecules will be evaluated.

PART ONE

Our unexpected results prompted a new investigation of the role of maspin in breast tumor progression. To further explore the clinical application of maspin in human cancer, it is critical to understand the in vivo biological function of maspin in tumor progression. To this end, ne of the most powerful models used to examine multistage carcinogenesis has been MMTV/TGF-α transgenic mouse. Elevated levels of TGF-α have been detected in transformed keratinocytes and in a variety of naturally occurring human tumor types (Gottlieb, 1988; Reddy, 1994). In addition, the role of TGF-α in neoplasia has been confirmed in a variety of experimental systems, including transgenic mice in which initially hyperplasia and later neoplasia of liver and mammary glands were observed (Jhappan, 1990; Matsui, 1990; Sandgren, 1990). In collaboration with Dr. Kaladhar Reddy at WSU, we evaluated the role of maspin as a tumor suppressor using MMTV/TGF-α transgenic mouse model.

MATERIALS AND METHODS

Generation and Characterization of MMTV/TGF-α Transgenic mice. The construction of MMTV LTR was similar to the previously published work of Matsui (Matsui, 1990). In brief, pMMTV/TGF-α, the SV40 early promoter region in the vector pKCR was replaced by the complete MMTV-LTR. A 925 bp human TGF-α cDNA (kindly provided by Dr. Bell, University of Chicago) was then inserted into EcoRI site of β-glonin exon 3. The 3.6 kb XhoI fragment was purified and microinjected into (C57BL X DBA) fertilized eggs. Homozygous TGF-α transgenic mice were obtained by breeding two heterozygous TGF-α transgenic mice. For histological examination of the mammary glands, the skin containing the mammary fat pads was fixed in 10% buffered formalin for at least 24 h. and then embedded in paraffin. Routinely, 5 μm sections of the whole mount tumor and mammary tissue were stained with hematoxylin and eosin using a standard protocol.

RNase Protection Assay. To confirm the expression of the TGF-α transgene, RNase protection assay was performed as described previously (Reddy, 1994). Briefly, the TGF-α probe used for RNase protection analysis was 152-bp SphI-ApaI fragment cloned in antisense orientation into pGEM7zf (provided by Dr. Kern, Lombardi Cancer Center, Washington, DC). The resulting plasmid was linearized with BamHI and transcribed with T7 polymerase in the presence of ^{32}P-labeled ATP. Thirty micrograms of total RNA from each sample were hybridized overnight at 50 °C with 50,000 cpm of probe in 30 μl of buffer containing 80% formamide, 40 mM piperazine-N,N'-bis(2-ethanesulfonic acid), 0.4 M NaCl, and 0.1 M EDTA. Samples were subsequently digested with 40 μg/ml RNase A (Sigma) for 30 min at 25 °C. Digestion was terminated with proteinase K and SDS. The samples were pelleted and resuspended in 5 μl of an 80% formamide loading buffer and run on 6% polyacrylamide sequencing gel with 8 M urea. Size markers were prepared by end labeling MspI-digested fragments of pBR322.

The gels were dried and exposed to X-ray film in the presence of an intensifying screen at −70 °C for 1 or 2 days.

Immunohistochemistry. The expression of maspin protein was immunostained by using AbS4A, a polyclonal antibody raised against the unique reactive loop sequence of maspin (Zou, 1994), on 5-μm sections cut from the aforementioned tissue blocks. The immunohistochemical staining was performed at room temperature unless otherwise stated for a specific step. The slides were deparaffinized in xylene and rehydrated in graded ethanols to PBS. Endogenous peroxidase activity was destroyed by treating the tissue for 10 minutes in 1% H_2O_2 in methanol. Antigen was retrieved in 10mM sodium citrate (pH 6.0) by microwave heating for 3 minutes in the case of surgical specimens and for 5 minutes on the whole mount autopsy tissues. Following the initial blocking with 10% normal goat serum for 30 minutes, the primary antibody was applied at 4.0 μg/ml with 1% BSA and 0.01% Triton-X100 and allowed to incubate overnight at 4°C. The tissues were then blotted with biotinylated anti-rabbit secondary antibody (Zymed) for 30 minutes, and subsequently with strepavidin-HRP (Zymed). The DAB color reaction was employed for detection according to the manufacturer's directions (Vector). The slides were counterstained with hematoxylin and dehydrated in a series of graded ethanols and xylene followed by mounting with Permount (Fisher). The negative controls of immunohistochemical staining were performed in the similar fashion except that purified preimmune IgG at a final concentration of 4 μg/ml was used in the place of Abs4A.

In-situ hybridization: The PCR-amplified full length coding sequence of maspin cDNA in the pGEM7Zf(+) vector (Xia, 2000) was used as the template for in vitro transcription with the DIG labeling kit (from Boehringer Mannheim, Indianapolis, IN). The resulting labeled full-length maspin mRNA was hydrolyzed to approximately 0.2 kb fragment, then used in the subsequent in situ-hybridization procedure. The DIG-labeled full-length sense strand maspin mRNA was used in parallel as the negative controls. The in situ hybridization was performed as described by the manufacturer with some modifications. Briefly, tissue specimens were deparaffinized in xylene and rehydrated through a series of graded ethanols to PBS. Following the permeabilization with 25μg Proteinase K in Tris/EDTA buffer (pH 8.0) for 30 minutes at 37 °C, the specimens were denatured with 4X SCC in 50% deionized formamide at 37°C for 10 minutes. The slides were then hybridized with 5-10 ng of DIG labeled probe overnight at 60 °C, followed by two washes with 0.1X SCC at 60 °C (with agitation). The specifically bound DIG-labeled DNA was detected by the color reaction of the horse-radish peroxidase-conjugated anti-DIG antibody. The sections are then counter stained with methyl green and mounted with Permount.

RESULTS:

TGF-α is a 50 amino acid 5.6 kDa secreted polypeptide that is cleaved from a large integral membrane glycoprotein. The matured TGF-α molecule shares 35% sequence homology with epidermal growth factor (EGF), binds to the same receptor, and has similar biologic effects (Derynck, 1988). A commonly cited action of both TGF-α and EGF is that they act as potent mitogens in a number of epithelial cell systems (Carpenter, 1979). Homozygous TGF-α transgenic mice

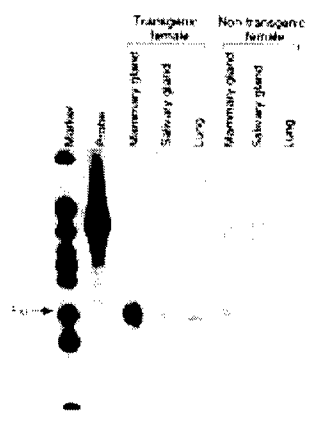

Figure 1. Targeted Expression of TGF-a in MMTV/TGF-α Transgenic Mice
Ribonuclease Protection Analysis of TGF-α transgene expression in various mouse tissues. Total RNA from mouse tissues was hybridized to uniformly labeled TGF-α probe, subjected to RNase digestion, electrophoresed in denaturing polyacrylamide gel, and exposed to autoradiographic film. The detected band was a fragment of TGF-α transgene.

were identified by southern blot analysis of tail DNA, and by 100% transmission of the gene when bread with non-transgenic mice (data not shown). In transgenic mice, TGF-α RNA expression was confirmed by RNase protection analyses. High levels of TGF-α expression were seen in mammary gland and a relatively low level of TGF-α was detected in sebaceous glands and lungs of transgenic multiparous females (Fig. 1). In contrast, age-matched non-transgenic multiparous females exhibited low levels of TGF-α expression in mammary glands and no signal in sebaceous gland and lung.

The mammary glands from transgenic or nontransgenic virgin females mice (4 weeks) showed no alveolar development. While the non-transgenic mice were not symptomatic throughout their lives, all 50 female transgenic mice used showed significant breast hyperplasia after multiple pregnancies. Twelve of these transgenic mice developed hyperkeratosis and bilateral lumps in their mammary glands. Histologic examination of whole mount tissues revealed significant alveolar hyperplasia throughout the entire mammary glands in the transgenic but not in nontransgenic mice (data not shown). Histologic examination revealed that some of the TGF-α- induced mammary tumors developed breast and sebaceous gland carcinoma as shown in Figure 2. Although these transgenic mice did no have distal metastases, five of them developed invasive breast carcinoma at 6-8 months of age, as shown in Figure 3.

Maspin Expression Inversely Correlates with the Mammary Tumor Progression in MMTV/TGF-α Transgenic Mice. In transgenic mouse group, each tumor specimen had multiple regions of hyperplasia and carcinoma *in situ*. Since the mammary tumors developed are rather small in size, it is very difficult to extract sufficient amount of either protein or RNA for quantitative comparison of maspin expression at a gross level by immunoblotting or Northern blotting. To investigate the expression and the localization of maspin protein in mouse breast tumor progression, we performed semi-quantitative immunohistochemical staining on the whole mount mammary tissues from 5 MMTV/TGF-α transgenic mice and 2 age-matched nontransgenic mice. Figure 2 shows representative immunohistochemical staining results. As can be seen, the oligopeptide-derived polyclonal antibody against maspin, Abs4A, exhibited a specific immunoreactivity with normal myoepithelial cells and normal luminal epithelial cells (Figure 2B). The parallel immunostaining with the preimmune serum gave rise to a negative staining pattern (Figure 2A). Furthermore, maspin expression appeared to be cytoplasmic in mammary epithelial cells and was not found in the stroma. As compared to normal mammary epithelium, mammary hyperplasia

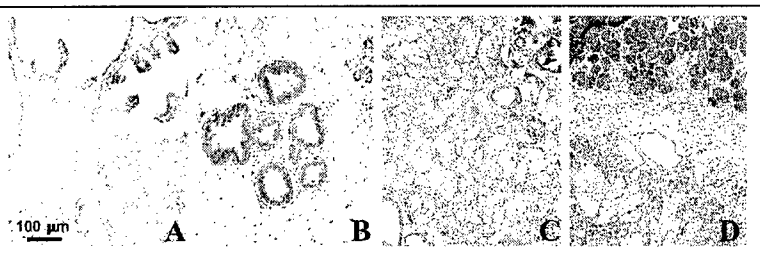

Figure 2. Immunohistochemical Staining of Maspin in the Mammary Gland of MMTV/TGF-α Transgenic Mice.

(**A**): Immunohistochemical staining of the nontransgenic mouse mammary tissue using the preimmune serum. (**B**): the high level expression of maspin in normal luminal and myoepithelial cells. (**C**): the moderate expression of maspin in hyperplastic mammary epithelial cells; (**D**): down-regulation of maspin in mammary carcinoma. The reddish brown-color represents positive maspin immunoreactivity. The cell nuclei are counter-stained blue. The white arrow in (**D**) indicates mammary carcinoma.

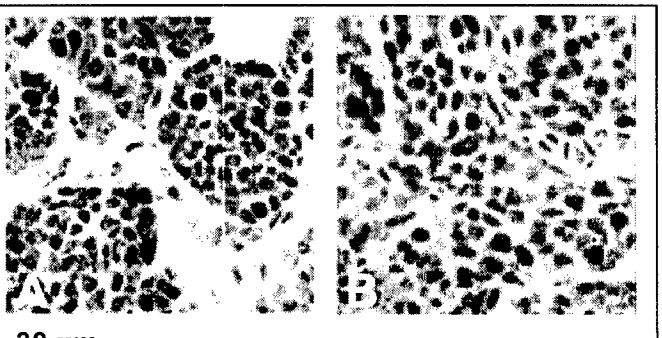

Figure 3. Maspin Expression Is Down-regulated in Invasive Mammary Carcinoma.

Microscopic examination at higher magnification shows maspin present in mammary carcinoma in situ (**A**), but lost in invasive mammary carcinoma (**B**) of TGF-α transgenic mice. Maspin detected by immunohistochemical staining gives rise to the reddish brown-color. The cell nuclei are counter-stained blue.

exhibited a moderate level of maspin expression (Figure 2C), while mammary carcinoma cells showed little or no maspin immunoreactivity (Figure 2D arrow). Microscopic examination using a higher magnification indicated that the loss of maspin expression was associated with invasive mammary carcinoma (Figure 3B). In all tumor samples from the transgenic group (5/5), consistent differential expression of maspin was observed.

To address whether maspin was specifically produced by mammary epithelial cells and whether maspin was differentially expressed at the mRNA level, in-situ hybridization was performed with the whole mount mammary tissues. While the sense-strand of maspin cDNA did not give rise to detectable signal (data not shown), a strong positive staining of maspin mRNA was detected in benign luminal and the myoepithelial cells. Hyperplastic mammary epithelium featured heterogeneous maspin staining of a moderate intensity. Mammary carcinoma in situ and invasive carcinoma cells expressed little or no maspin mRNA. The stroma of both transgenic and non-transgenic mouse mammary glands was free of maspin mRNA signal. Our TGF-alpha transgenic mice showed a range of abnormalities in the mammary gland including lobular hyperplasia, different stages of tumor progression in the same tumor such as hyperplasia (ductal or lobular), carcinoma in situ, or invasive carcinoma. adenomas, hyperkeratosis and mammary carcinoma. Using a combination of immunohistochemistry and *in situ* hybridization, we show that both normal myoepithelial cells and normal ductal epithelial cells express maspin at a high level. Hyperplastic mammary epithelium and mammary carcinoma in situ (DCIS) expressed a moderate level of maspin. However more malignant stage of tumors such as invasive carcinoma show a significant reduction or total loss of maspin.

CONCLUSION: In conclusion, we found a direct correlation between down-regulation of maspin expression and the stage of mammary tumors in MMTV/TGF-*a* transgenic mice. Our data suggests that MMTV/TGF-α transgenic mouse model is advantageous for *in vivo* evaluation of both the expression and the biological function of maspin during the slow mutli-stage carcinogenesis of mammary gland.

PART TWO

We started to generate DNA constructs for experssiong of recombinant maspin and maspin-derived mutant proteins in baculovirus system.

Current evidence supports the role of maspin as a serine proteinase inhibitor. The primary protein sequence and the predicted general structural framework of maspin are similar to those of the inhibitory serpins and are consistent with the functional evidence that the tumor suppressive activity of maspin depends on its intact RSL. To elucidate the structural-functional relationship of maspin, three maspin mutants have been successfully overexpressed using a baculo-virus expression system (Pharmingen). Modified heparin column chromatography procedures were developed to purify these maspin variants (Figure 4).

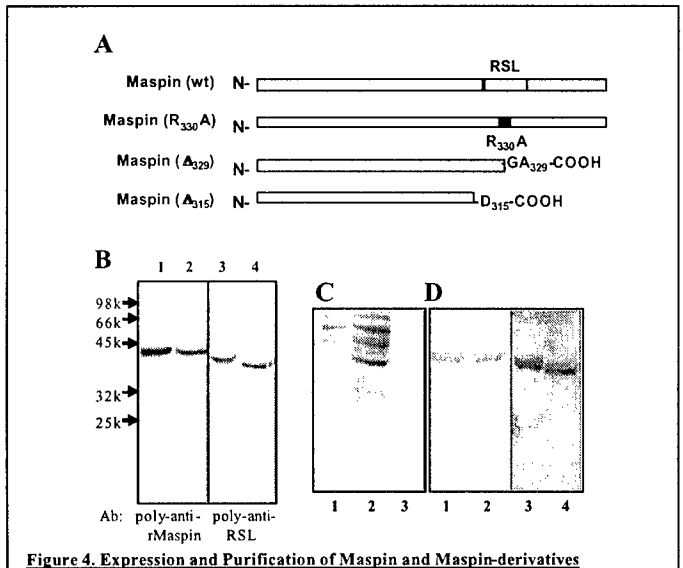

Figure 4. Expression and Purification of Maspin and Maspin-derivatives
(A): schematic structures of three maspin-derived polypeptides; (B): Western blot of maspin and maspin-derivatives expressed by baculo virus-infected *Sf9* insect cells. Lanes 1-4 are the lysates of cells expressing wild type Maspin, Maspin(R330A), Maspin (ΔCT329), and Maspin(ΔCT315), respectively. Lanes1 and 2 were detected by Abs4A, while lanes 3 and 4 were detected by a polyclonal antibody against recombinant wild type maspin (Pharmingen). (C): Purification of maspin by heparin-affinity chromatography followed by Coomassie blue stained SDS-PAGE. Lane 1 is the lysate of uninfected insect cells . Lane 2 is the lysate of Sf9 cells infected with maspin-expressing baculo virus. Lane 3 is purified Maspin. (D) Purified maspin-derivatives analyzed by SDS-PAGE followed by Coomassie blue staining. Lanes 14 are type Maspin,. Maspin(R330A), Maspin(ΔCT329), andMaspin(ΔCT315),respectively.

PART THREE

Continue to Characterization of Maspin in drug-induced apoptosis using stable transfectants-derived from breast Carcinoma cells MDA-MB-435 that express maspin, maspin/PAI-1 and PAI-1/maspin, respectively.

MATERIALS AND METHODS

Induced Apoptosis. Cells cultured in 6-well plates for 24 were incubated with 0.5 μM STS at 37 °C with 6.5 % CO_2 for indicated hours. To test the effect of secreted maspin, STS was added to the cells that had been cultured for 24 hours in the K-SFM pre-conditioned (for 24 hours) by maspin transfectants or pCIneo cells. To examine the effect of purified recombinant human maspin (rMaspin) cells were incubated with rMaspin at a final concentration of 20-200 nM for 24 hr prior to the addition of STS.

TUNEL Assay and Electrophoresis Assays for DNA Fragmentation.

To detect DNA fragmentation at the cellular level, cells were seeded in 8-well Lab-Tek®II chamber slides at a density of 100,000/well and incubated for 24 hours in the corresponding maintenance media. The cells were treated with 0.5 μM STS 24 hours (with the exception of 12 hours for 70N cells), washed twice with PBS and fixed with freshly prepared 4% paraformaldehyde at room temperature for 25 minutes. The cells were washed and permeabilized in 0.2% Triton X-100 (in PBS) for 5 minutes at room temperature. The cells were then washed and stained by a modified TUNEL procedure using the DeadEnd™ Colorimetric Apoptosis Detection System (Promega, Madison, WI).

To detect DNA fragmentation at the molecular level, cells were seeded in 60 mm petri dishes at a density of 2 x 10^6/dish and incubated in the corresponding media for 24 hours before the STS treatments. DNA isolated from either STS-treated of untreated cells using the Apoptotic DNA ladder Kit (Roche Diagnostics GmbH, Mannheim, Germany) were analyzed by 1% agarose gel electrophoresis and visualized by ethidium bromide fluorescent staining.

Caspase Activity Assays. For caspase-3 activity assay, cells were treated with STS for 4 hr. For caspase-8 activity assay, cells were treated with STS for 2 hr. Following the removal of detached cells by aspirating the culture media, the remaining adherent cells were lysed in 200 μl of 50 mM Tris buffer (pH 7.5) containing 0.05% Nonidet and 1 mM DTT. The clear supernatant (cytosolic fraction) resulting from the centrifugation at 12,000 g for 5 minutes at 4°C was collected. A total of 25 μg protein from each cytosolic fraction was incubated with 40 μM peptide substrate for caspase-3, or caspase-8 for 120 min at 37 °C in 200 μl reaction mixtures containing 10 mM HEPES (pH 7.5), 50 mM NaCl, and 2.5 mM DTT. The peptide substrates for caspase-3 and caspase-8 were Ac-DEVD-AMC and Ac-IETD-AMC, respectively (International Bio, CA). To test the effect of purified maspin on caspase-3 activity, rMaspin was added at 20-200 nM final concentrations along with the fluorogenic substrate of caspase-3 into the assay mixtures. Fluorescence released by caspase activity was measured at 380 $nm_{excitation}$ and 460 $nm_{emission}$ using the SPECTRAmax GEMINI spectrofluorometer (Molecular Devices, CA). The cytosolic fractions of untreated cells were analyzed in parallel and were used as the background.

RESULTS

The apoptotic effect of STS was further evaluated by a modified TdT-mediated dUTP Nick-End Labeling (TUNEL) assay. When the mock control cells were treated with STS in the range of 05 to 2 μM for 24 hours, a dose-dependent apoptosis was observed. In all subsequent experiments, cells were treated with 0.5 μM STS, a minimum concentration to induce detectable DNA fragmentation in the pCIneo cells. As shown in Figure 5, the pCIneo cells showed significant shrinkage that is typical for STS-induced apoptosis (Gomez-Angelats M, 2000; Jacobsen MD, 1996; Tang D, 2000)

However, only a small fraction (10 ± 2.4%) of this cell population gave rise to a detectable TUNEL reactivity. In parallel, STS treatment of maspin-expressing transfectant clone Tn15 led to not only cell shrinkage, but also a high level of DNA fragmentation in 54 ± 5.5% of the total cell population. STS treated Tn16 and three other maspin transfectant clones exhibited a TUNEL reactivity comparable to that of STS treated Tn15 (data not shown). Interestingly, normal mammary epithelial cells 70N that express maspin at a high level (Zou, 1994) were even more sensitive to STS-induced apoptosis than Tn15 (and Tn16) cells. In fact, treatment of 70N cells with 0.5 μM STS for 24 hours lead to complete cell detachment and death (data not shown). When treated with 0.5 μM STS for 12 hours, 70N cells remained largely adherent, but showed a high level of DNA fragmentation, comparable to that found in STS-treated Tn15 cells (for 24 hours).

To verify the differential DNA fragmentation patterns among different cell lines at the molecular level, total DNA was isolated from pCIneo cells and maspin transfectant clones. As shown in Figure 6A, little or no DNA fragmentation was detected in all untreated cell lines. STS treatment led to marginal DNA fragmentation in pCIneo cells. In contrast, STS-treated Tn15 (and Tn16, data not shown) and 70N cells gave rise to fragmented DNA at a significantly elevated level. Western blot analysis showed (Figure 6B) that pCIneo cells, both untreated and STS-treated, expressed no detectable maspin. On the other hand, the constitutively expressed maspin in transfectant clones was not altered by STS-induced apoptosis.

A hallmark of cellular response to apoptotic DNA fragmentation is the inactivation of poly-[ADP-ribose]-polymerase (PARP), an enzyme that catalyzes nuclear protein ribosylation and facilitates DNA damage repair (Bromme HJ, 1996). The inactivation of the 116 kDa PARP is carried out by specific proteolytic

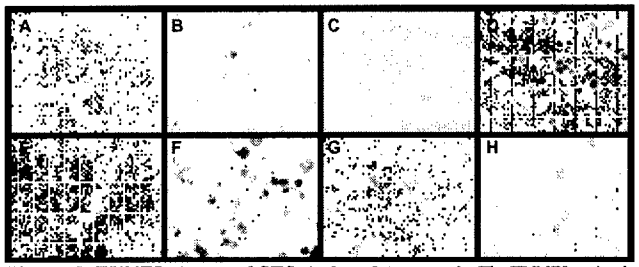

Figure 5. TUNEL Assay of STS -induced Apoptosis. The TUNEL stained cells were viewed and counted with a Lica microscope (model DM-IRB) and the pictures were acquired using an attached SPOT II digital camera. x400. The dark color co-localizing with nuclei represents TUNEL positive stain (converted to gray scale from the original brown color). The TUNEL positive cells in each sample were counted in 10 random fields and were presented as a percentage of the total number of cells counted (the number in parentheses). (**A**), untreated pCIneo (2.3 ± 1.7%); (**B**), STS-treated pCIneo cells (10 ± 2.4%); (**C**), untreated 70N cells (2.0 ± 1.2%; **D**, STS-treated 70N cells (44 ± 3.6%); (**E**), untreated Tn15 cells (2.7 ± 2.0%); (**F**), STS-treated Tn15 cells (54 ± 5.5%); (**G**), STS-treated maspin/PAI-1 transfectant clone #12 (19 ± 4.5%); (**H**), STS-treated PAI-1/maspin transfectant clone #5 (13 ± 2.0%). The untreated maspin/PAI-1 and PAI-1/maspin transfectants appeared similar to untreated Tn15 (data not shown).

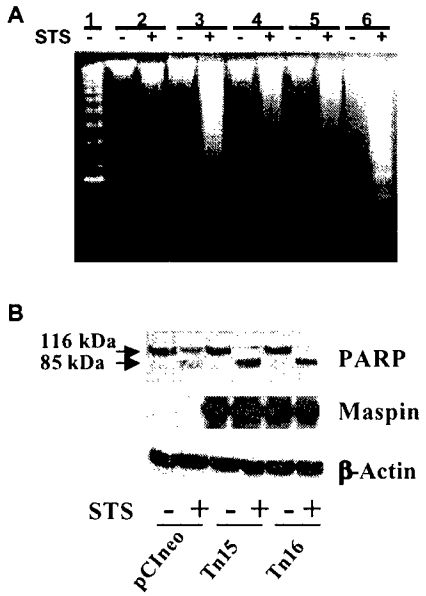

Figure 6. DNA Fragmentation and PARP Inactivation. (**A**) Agarose gel electrophoresis of DNA ladder. Lane 1 shows the DNA molecular weight marker. Samples 2-6 represent DNA isolated from untreated and STS-treated pCIneo, Tn15, Maspin/PAI-1 clone # 12, PAI-1/maspin transfectant clone #5, and normal mammary epithelial cells 70N, respectively. A total of 10 μg of DNA was loaded into each lane. (**B**) Western blotting of PARP and maspin. Cells were incubated in serum-free medium in the presence or absence of STS for 24 hours, and then lysed. A total of 100 μg of lysate protein from each cell line was resolved by SDS-PAGE and transferred to PVDF membrane, which was then probed with specific antibodies against PARP. The same blot was stripped and re-probed with the specific antibody against maspin. To assess the loading normality, the same blot was subsequently re-probed with the antibody against β-actin.

cleavage, yielding an 85 kDa PARP fragment (Boulares AH, 1999; D'Amours D, 1998). As shown in Figure 5B, the conversion of PARP from 116 kDa to 85 kDa was significantly increased in Tn15 and Tn16 cells as compared to that in pCIneo cells. This data further confirms that maspin expression indeed sensitized cells to STS-induced cell death via an apoptotic mechanism. Taken together, endogenous maspin expression was not sufficient to cause spontaneous cell death. However, it sensitized MDA-MB-435 cells to STS-induced apoptosis.

CONCLUSION:

We confirmed the sensitizing effect of endogenous maspin in STS-induced apoptosis at both the cellular level and molecular level. Furthermore, in TUNEL assay, DNA fragmentation assay and PARP degradation analyses, maspin/PAI-1 and PAI-1/maspin lost the sensitizing effect as compared to the wild-type maspin.

PUBLICATION

Reddy KB, McGowen R, Schuger L, Visscher D, Sheng S. Maspin expression inversely correlates with breast tumor progression in MMTV/TGF-alpha transgenic mouse model. Oncogene 2001 Oct 4;20(45):6538-43.

MANUSCRIPT IN PREPARATION

Ning Jiang, Yonghong Meng, Suliang Zhang, Edith Mensah-Osman, and Shijie Sheng, Maspin Sensitizes Breast Carcinoma Cells to Induced Apoptosis. Oncogene, (in revision)

REFERENCES

Boulares AH, Yakovlev AG, Ivanova V, Stoica BA, Wang G, Iyer S, Smulson M. (1999). *J Biol Chem*, 274(22932-40.

Bromme HJ, Holtz J. (1996). *Mol Cell Biochem*, 163-164, 261-75.

Carpenter, G, Cohen, S. (1979). *Annu. Rev. Biochem.*, 48, 193-216.

D'Amours D, Germain M, Orth K, Dixit VM, Poirier GG. (1998). *Radiat Res*, 150, 3-10.

Derynck, R. (1988). *Cell*, 54, 593-595.

Gomez-Angelats M, Bortner CD, Cidlowski JA. (2000). *J Biol Chem*, 275, 19609-19.

Gottlieb, AB, Chang, CK, Posnett, DN, Fanelli, B, Tam, JP. (1988). *J. Exp. Med.*, 167, 670-675.

Jacobsen MD, Weil M, Raff MC. (1996). *J Cell Biol*, 133, 1041-51.

Jhappan, C, Stahle, C, Harkins, RN, Fausto, N, Smith, GH, Merlino, GT. (1990,). *Cell*, 61, 1137-1146.

Matsui, Y, Halter, SA., Holt, JT, Hogan, BL, Coffey, RJ. (1990). *Cell*, 61, 1147-1155.

Reddy, KB, Yee, D, Hilsenbeck, SG, Coffey, RJ, Osborne, CK. (1994). *Cell Growth Differ*, 5, 1275-1982.

Sandgren, EP, Luetteke, NC, Palmiter, RD, Brinster, RL, Lee, DC. (1990). *Cell*, 61, 1121-1135.

Tang D, Lahti JM, Kidd VJ. (2000). *J Biol Chem*, 275, 9303-7.

Xia, W, Lau, YK, Hu, MC, Li, L, Johnston, DA, Sheng, S, El-Naggar, A, Hung, MC. (2000). *Oncogene*, 19, 2398-2403.

Zou, Z., Anisowicz, A., Hendrix, M. J. C., Thor, A., Neveu, M., Sheng, S., Radfidi, K., Seftor, E., and Sager, R. (1994). *Science*, 263, 536-529.